

Supplemental information: Online monitoring of Lanthanide species with combined spectroscopy in flowing aqueous aerosol systems

Garrett LeCroy,^{a,‡} Qiufeng Yang,^{a,‡} Micah Raab,^b Ruchi Gakhar,^{*,a} and Ammon Williams,^{*,b}

^a *Advanced Technology of Molten Salts, Idaho National Laboratory, Idaho Falls, Idaho 83415 USA*

^b *Material Minimization, Security & International Safeguards Department, Idaho National Laboratory, Idaho Falls, Idaho, 83415, US*

[‡] G.L. and Q.Y. contributed equally to this work

E-mail: ruchi.gakhar@inl.gov; ammon.williams@inl.gov

Contents

1	Supplemental Methods	2
2	Supplemental Figures	3
2.1	Steady-state absorption spectra during spike testing	3
2.2	Select LIBS emission peaks for calibration sample 12 with mixed Nd and Pr species	4
2.3	Possible flow disturbance in absorption cell	5
2.4	Use of absorption and LIBS data separately for real-time spike-test monitoring	6

1 Supplemental Methods

Time Synchronization of absorption spectroscopy and LIBS data during spiking tests

As outlined in the Methods section of the main text, absorption spectra during the spike testing of the process fluid were collected approximately every 1.2 minutes while LIBS spectra were collected every 0.5 minutes. The two sets of spectral data needed to be time synchronized for use in the combined multivariate analysis used in the main text. To accomplish this, LIBS spectra were linearly interpolated in the first order to match the time stamps associated with the absorption spectroscopy data. Each absorption spectrum had an associated time stamp, t_{abs} that corresponds to an absorbance spectral intensity, $A(t_{\text{abs}}, \lambda)$, and each LIBS spectra had an associated time stamp t_{LIBS} that corresponds to a LIBS emission intensity, $E(t_{\text{LIBS}}, \lambda)$. The linearly interpolated LIBS emission intensity at t_{abs} is $E(t_{\text{abs}}, \lambda)$ as give by Equation 1:

$$E(t_{\text{abs}}, \lambda) = E(t_{\text{LIBS}}^{n-1}, \lambda) + (E(t_{\text{LIBS}}^{n+1}, \lambda) - E(t_{\text{LIBS}}^{n-1}, \lambda)) \times \left(\frac{t_{\text{abs}} - t_{\text{LIBS}}^{n-1}}{t_{\text{LIBS}}^{n+1} - t_{\text{LIBS}}^{n-1}} \right) \quad (1)$$

where t_{LIBS}^{n-1} represents the time stamp of the LIBS spectrum collected closest to but not exceeding t_{abs} (i.e., the time stamp of the LIBS spectrum immediately preceding t_{abs} such that $t_{\text{LIBS}}^{n-1} < t_{\text{abs}}$), t_{LIBS}^{n+1} represents the time stamp of the LIBS spectrum collected closest to but not less than t_{abs} (i.e., the time stamp of the LIBS spectrum immediately following t_{abs} such that $t_{\text{LIBS}}^{n+1} > t_{\text{abs}}$), and $E(t_{\text{LIBS}}^n, \lambda)$ represents the LIBS emission intensity collected at time t_{LIBS}^n at wavelength λ .

2 Supplemental Figures

2.1 Steady-state absorption spectra during spike testing

During spike testing of the process fluid, the process fluid was allowed to homogenize after the spike additions. This homogenization was monitored using the absorption flow cell (see Figure 1 of main text) and the process fluid was taken as homogeneous when three subsequent absorbance scans displayed negligible changes (i.e., spectra represented a steady-state solution). At that point, samples were collected from the process fluid for offline ICP-MS analysis. The resulting steady-state spectra are shown in Figure S1.

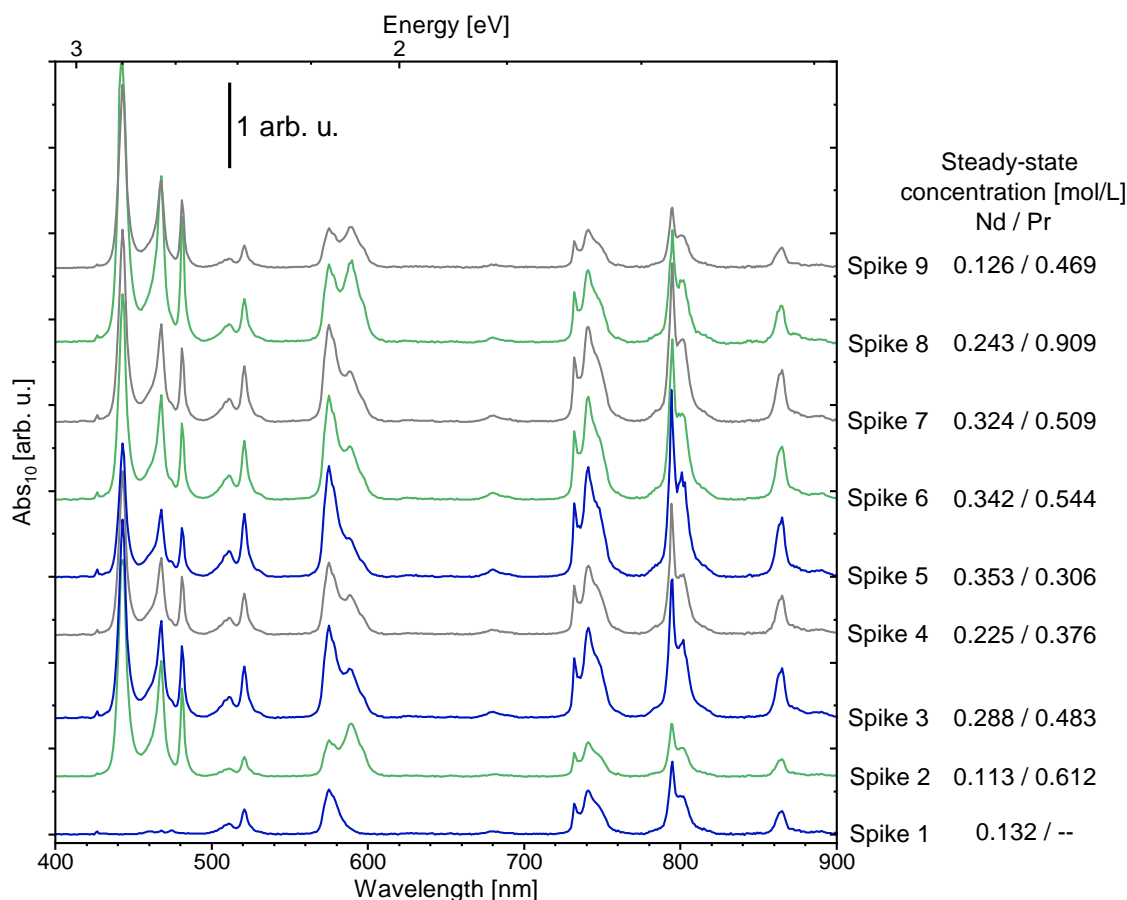


Figure S1: Absorption spectra collected during spike testing at steady-state conditions. These spectra correspond to the spectra taken at the points of ICP-MS sample collection shown in Figure 8 of the main text (see the black dots and pink squares in Figure 8). Spectra are arbitrarily offset for viewing clarity but are not normalized. Concentrations of Nd and Pr listed to the side of each spectra represent ICP-MS results. Blue traces (—) correspond to spectra collected after adding spikes of NdCl_3 containing solutions, green traces (—) correspond to spectra collected after adding spikes of PrCl_3 containing solutions, and gray traces (—) correspond to spectra collected after adding spikes of 2% v/v HNO_3 (i.e., blank) solutions. Corresponding spike number labels are shown (see Table 2 of main text), along the resulting steady-state process fluid concentration as found from offline ICP-MS analysis.

2.2 Select LIBS emission peaks for calibration sample 12 with mixed Nd and Pr species

Select LIBS emission peaks from calibration sample 12 (0.146 mol/L Nd and 0.293 mol/L Pr, see Table 1 of main text) are shown in Figure S2. Corresponding emission peak labels of select peaks are shown based on assignment from the NIST atomic spectra database.¹

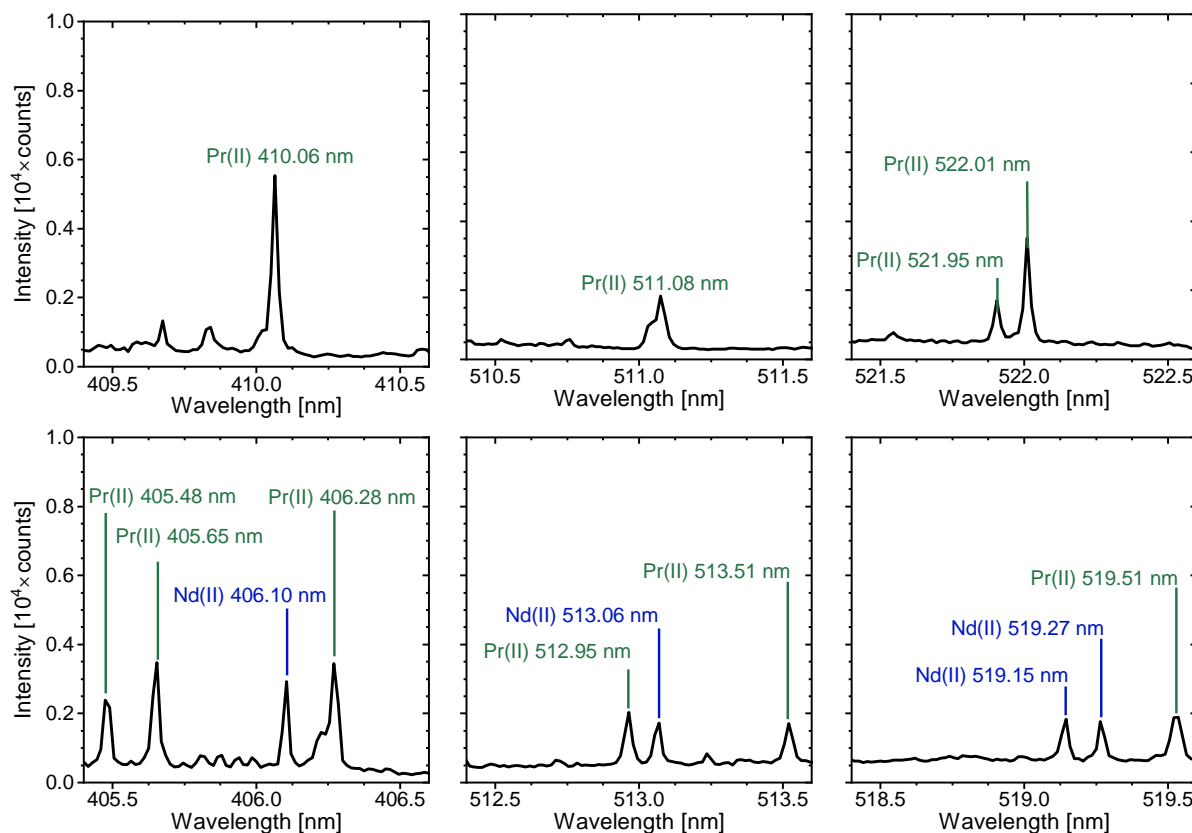


Figure S2: Select LIBS emission peaks from calibration sample 12 (0.146 mol/L Nd and 0.293 mol/L Pr, Table 1 of main text). Emission labels with experimental emission wavelength and atomic ionization state are shown. Data shown is unnormalized. The ordinate remain the same across all panels.

2.3 Possible flow disturbance in absorption cell

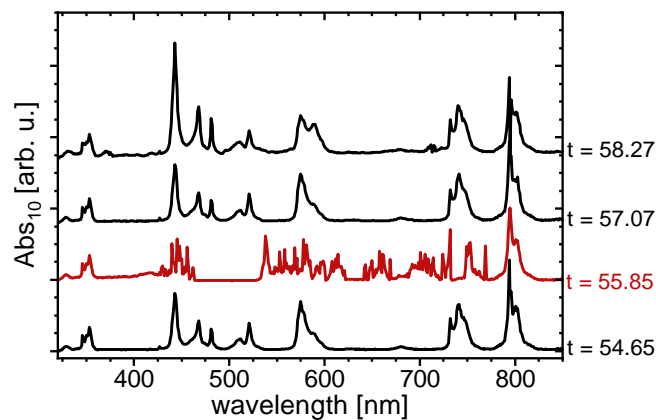


Figure S3: Raw absorbance data collected from the absorbance flow cell (Figure 1 of main text) at several time (t) collection points in minutes surrounding the anomalous predicted Pr^{3+} concentration highlighted in Figure 8 of the main text. Times are shown in minutes. The time at $t = 55.85$ minutes (highlighted red) shows a clear disturbance in absorbance measurement, with key Pr^{3+} absorbance peaks in the 430–480 nm region obscured or missing. We hypothesize that this is the result of a trapped gas bubble traveling through the absorbance flow cell. The system appears to stabilize quickly, with absorbance readings on either side of $t = 55.85$ minutes not displaying this pronounced disturbance.

2.4 Use of absorption and LIBS data separately for real-time spike-test monitoring

Figure 8 of the main text shows the use of a combined, multivariate regression model based on both absorption and LIBS data to provide real-time monitoring of a process fluid during intermittent spike-testing. Figure S4 shows the use of either an absorption multivariate regression model or a LIBS multivariate regression model separately (see main text for discussion of models). Predictions based on LIBS data are seen to lag slightly behind those of absorption spectroscopy in the first ≈ 40 minutes of testing, likely due to the LIBS data collection being positioned downstream from absorption spectroscopy characterization (see Figure 1 of the main text and discussion around Figure S5). However, the separate results show little time lag (estimated less than 3 minutes at maximum time lag) between predictions based on absorption spectroscopy and separate predictions based on LIBS emission data. This is an encouraging result for the use of combined spectroscopic characterization of process fluids, by highlighting that optical characterization need not necessarily take place at the same place in the fluid stream.

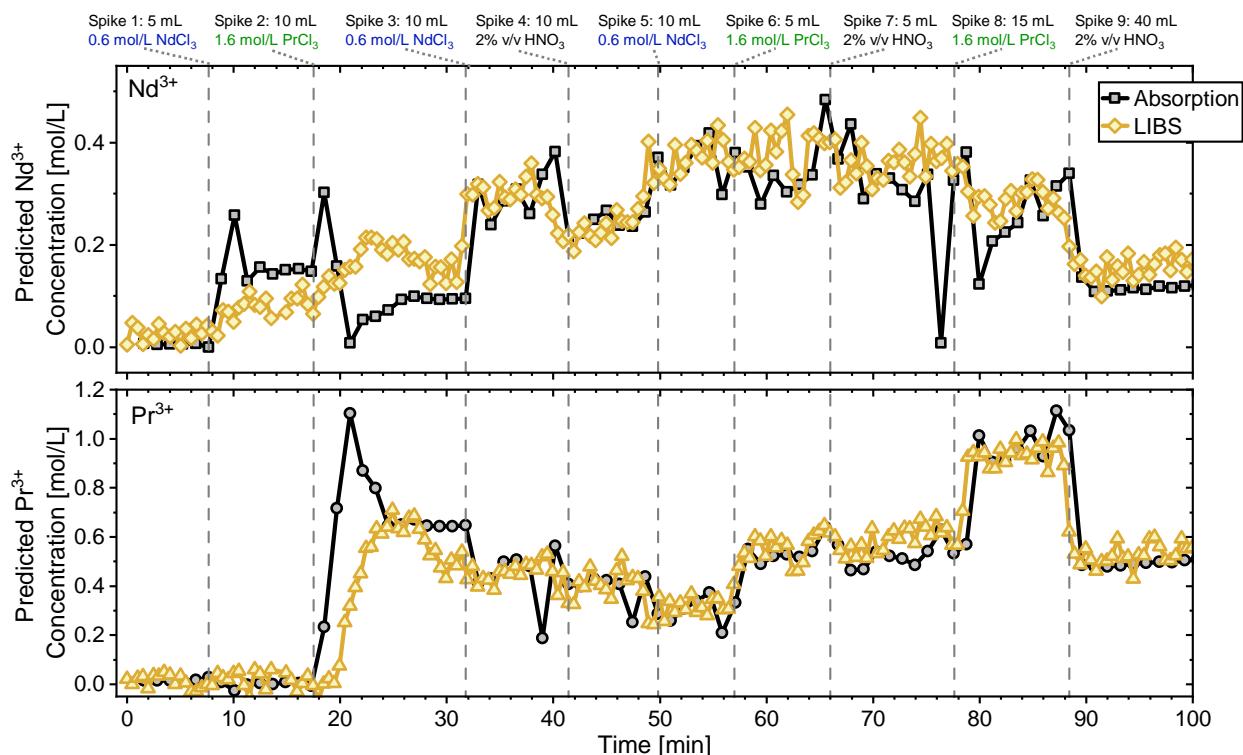


Figure S4: Comparison of multivariate model predictions for (top panel) Nd and (bottom panel) Pr concentration as a function of time during spike testing as monitored by absorption spectroscopy or LIBS separately. The abscissa remains constant across both panels. Times of spike addition are shown with vertical dashed lines, and corresponding spikes are shown on top of figure.

2.4.1 Simplified model of fluid flow

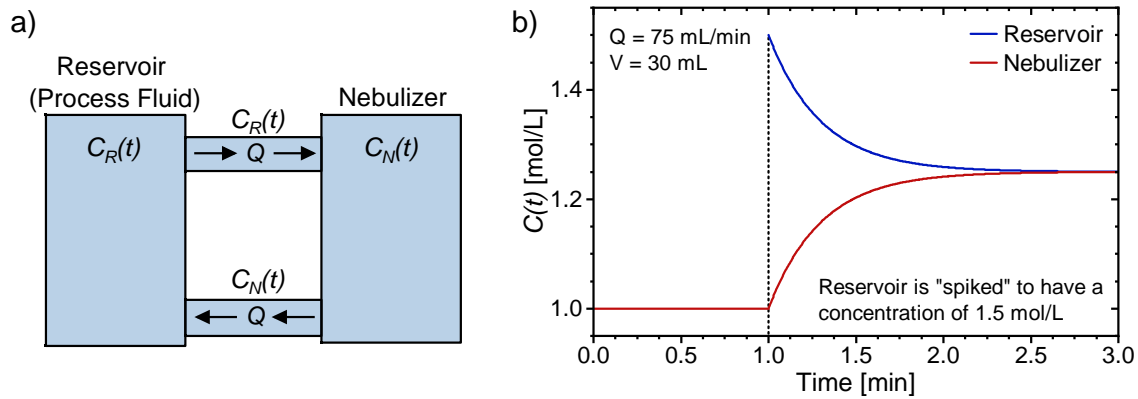


Figure S5: (a) Simplified schematic of fluid flows between the process fluid reservoir and the nebulizer (see Figure 1 of main text). The absorption flow-cell would measure on the fluid transfer from the reservoir to the nebulizer. Concentrations of arbitrary analytes, $C_R(t)$ and $C_N(t)$, are shown for the reservoir and nebulizer respectively. Q denotes fluid volume flow rates between the two containers. (b) simulated analyte concentration changes in the reservoir and nebulizer for an event where the fluid is initially at a steady-state analyte concentration of 1 mol/L, and then a sudden spike occurs at time $t = 1$ min where the analyte concentration the reservoir is changed to 1.5 mol/L. Fluid mass flow rate and volume, V , of the fluid in the reservoir and nebulizer are shown where both the reservoir and nebulizer have a starting volume of 30 mL of solution each.

Figure S5a shows a highly-idealized view of fluid flows in the sampling system shown in Figure 1 of the main text. The process fluid reservoir and nebulizer have concentrations of an arbitrary analyte of $C_R(t)$ and $C_N(t)$ respectively. There are fluid volume flow rates of Q that move fluid from the reservoir to the nebulizer and then back from the nebulizer to the reservoir. The time lag in prediction results based on LIBS from those of absorption spectroscopy (see discussion around Figure S4), along with the qualitatively "smoother" concentration changes seen in predictions from LIBS data can be interpreted based on the relative placement of the LIBS measurement compared with the absorption flowcell. The following simplifying assumptions are taken to provide an approximate understanding of these phenomena.

Simplifying assumptions for fluid flow calculations

1. The fluid flow rate between the reservoir and nebulizer and the return flowrate are equivalent
2. The reservoir and nebulizer containers are each homogeneous at all times (i.e., there is no change of analyte concentrations with respect to position in either the reservoir or nebulizer)
3. Solution spikes in the reservoir lead to an instantaneous, homogeneous change of solution concentration in the reservoir.
4. The fluid flow leaving either the nebulizer or reservoir has the same concentration as the homogeneous nebulizer or reservoir.
5. The loss of material from aerosol generation is negligible
6. The volumes of fluid in the reservoir (V_R) and nebulizer (V_N) are equivalent at a constant V

Starting with these assumptions, a set of coupled first-order differential equations can be written for the concentrations of an arbitrary analyte as functions of time, t , in the reservoir, $C_R(t)$, and the nebulizer, $C_N(t)$, shown in Equations 2 and 3, respectively.

$$\frac{V}{Q} \frac{dC_R(t)}{dt} = C_N(t) - C_R(t) \quad (2)$$

$$\frac{V}{Q} \frac{dC_N(t)}{dt} = C_R(t) - C_N(t) \quad (3)$$

Taking the steady-state boundary conditions as $C_R(t = \infty) = C_N(t = \infty) = C_{\text{steady-state}}$, Equations 2 and 3 can be solved to yield Equations 4 and 5:

$$C_R(t) = (C_R(t=0) - C_{\text{steady-state}}) \exp(-2tQ/V) + C_{\text{steady-state}} \quad (4)$$

$$C_N(t) = (C_N(t=0) - C_{\text{steady-state}}) \exp(-2tQ/V) + C_{\text{steady-state}} \quad (5)$$

The rate at which either the reservoir or nebulizer reaches steady-state is essentially dependent on the ratio of flowrate between the reservoir and nebulizer and the volume in either container (Q/V). A simulated example of analyte concentration changes are shown in Figure S5b under the conditions of $Q = 75$ ml/min, $V = 30$ mL, both the reservoir and nebulizer have initial analyte concentrations of 1 mol/L, and at a time of $t = 1$ min, the reservoir is spiked to yield a sudden concentration of 1.5 mol/L in the reservoir. The simplified simulation shown in Figure S5b shows that the concentration spike takes time to propagate to the aerosol nebulizer, but the spike will be monitored by the absorption flowcell placed on the uptake from the reservoir much more quickly.

Notes and references

- [1] A. Kramida, Y. Ralchenko, J. Reader and N. A. Team, *NIST Atomic Spectra Database*, 2025, <https://physics.nist.gov/asd>.